THE SIMPLEST MIXED FINITE ELEMENT METHOD FOR LINEAR ELASTICITY IN THE SYMMETRIC FORMULATION ON n-RECTANGULAR GRIDS

JUN HU, HONGYING MAN, AND SHANGYOU ZHANG

Abstract. A family of mixed finite elements is proposed for solving the first order system of linear elasticity equations in any space dimension, where the stress field is approximated by symmetric finite element tensors. This family of elements has a perfect matching between the stress components and the displacement. The discrete spaces for the normal stress σ_{ii}, the shear stress σ_{ij} and the displacement u_i are span$\{1, x_i\}$, span$\{1, x_i, x_j\}$ and span$\{1\}$, respectively, on rectangular grids. In particular, the definition remains the same for all space dimensions. As a result of these choices, the theoretical analysis is independent of the spatial dimension as well. In 1D, this element is nothing else but the 1D Raviart-Thomas element, which is the only conforming element in this family. In 2D and higher dimensions, they are new elements but of the minimal degrees of freedom. The total degrees of freedom per element is 2 plus 1 in 1D, 7 plus 2 in 2D, and 15 plus 3 in 3D. The previous record of the least degrees of freedom is, 13 plus 4 in 2D, and 54 plus 12 in 3D, on the rectangular grid. These elements are the simplest element for any space dimension.

The well-posedness condition and the optimal a priori error estimate of the family of finite elements are proved for both pure displacement and traction problems. Numerical tests in 2D and 3D are presented to show a superiority of the new element over others, as a superconvergence is surprisingly exhibited.

Keywords. First order system, symmetric stress field, mixed finite element, nonconforming finite element, inf-sup condition.

AMS subject classifications. 65N30, 73C02.

1. Introduction

The first order system of equations, for the symmetric stress field $\sigma \in \Sigma := H(\mathrm{div}, \Omega, \mathbb{S})$ and the displacement field $u \in V := L^2(\Omega, \mathbb{R}^n)$, reads: Find $(\sigma, u) \in \Sigma \times V$ such that

$$(1.1)\qquad \begin{aligned} (A\sigma, \tau) + (\mathrm{div}\tau, u) &= 0 \qquad && \forall \tau \in \Sigma, \\ (\mathrm{div}\sigma, v) &= (f, v) && \forall v \in V. \end{aligned}$$

Here the symmetric tensor-valued stress space Σ and the vector-valued displacement space V are, respectively,

$$(1.2)\qquad H(\mathrm{div}, \Omega, \mathbb{S}) = \Big\{ \big(\sigma_{ij}\big)_{n\times n} \in H(\mathrm{div}, \Omega) \ \Big|\ \sigma_{ij} = \sigma_{ji} \Big\},$$

$$(1.3)\qquad L^2(\Omega, \mathbb{R}^n) = \Big\{ \big(u_1, \ \ \cdots, u_n\big)^T \ \Big|\ u_i \in L^2(\Omega) \Big\}.$$

In 1D, one example of the problem (1.1) is the mixed formulation of the 1D Poisson equation; In 2D and 3D, the stress-displacement formulation based on the Hellinger-Reissner principle for the linear elasticity can be regarded as a celebrated example of (1.1).

Because of the symmetry constraint on the stress tensor, $\sigma_{ij} = \sigma_{ji}$, it is extremely difficult to construct stable conforming finite elements of (1.1) even if for 2D and 3D, as stated in the plenary presentation to the 2002 International Congress of Mathematicians by D. N. Arnold. Hence compromised works use composite elements [6, 22], or enforce the symmetry condition weakly [2, 5, 11, 24, 27, 28, 29]. The landmarks in this direction are the respective works of Arnold and Winther [8] and Arnold, Awanou, and

The first author was supported by the NSFC Project 11271035, and in part by the NSFC Key Project 11031006.

Σ_K :	$\{1, x, y, y^2, xy\}$	$\{1, x, y, x^2, y^2\}$	$\{1, x\}$	$\{1, x, y\}$
	$\{1, x, y, x^2, y^2\}$	$\{1, x, y, xy, x^2\}$	$\{1, x, y\}$	$\{1, y\}$
V_K :	$\{1, y\}$	$\{1, x\}$	$\{1\}$	$\{1\}$

FIGURE 1. 2D elements by Hu-Shi [21], Yi [31] and this paper.

Winther [4]. In particular, a sufficient condition of the discrete stable method is proposed in these two papers, which states that a discrete exact sequence guarantees the stability of the mixed method. Based on such a condition, conforming mixed finite elements on the simplicial and rectangular triangulations are developed for both 2D and 3D [1, 3, 4, 8]. In order to keep conformity the vertex degrees of freedom are in particular employed in these conforming methods. To avoid the complexity of conforming mixed element and also vertex degrees of freedom, new weak-symmetry finite elements [7, 16, 18, 19], non-conforming finite elements [9, 21, 17, 23, 30, 31] are constructed. See also [15, 10] for the enrichment of nonconforming elements of [21, 23] to conforming elements. However, most of these elements are difficult to be implemented; numerical implementation can only be found in [13, 14, 31] so far, all in 2D.

Σ_K :	$\{1, x\}$	$\{1, x, y\}$	$\{1, x, z\}$
	$\{1, x, y\}$	$\{1, y\}$	$\{1, x, z\}$
	$\{1, x, z\}$	$\{1, y, z\}$	$\{1, z\}$
V_K :	$\{ 1 \}$	$\{ 1 \}$	$\{ 1 \}$

FIGURE 2. The 3D element of this paper.

In this paper, a new family of minimal, any space-dimensional, symmetric, nonconforming mixed finite elements for the problem (1.1) is constructed. It is motivated by a simple fact that, by (1.2), the derivative on a normal stress component σ_{ii} is only in x_i direction; while those on σ_{ij} are only in x_i and x_j directions. Thus, the minimal finite element space for σ_{ii} would be span$\{1, x_i\}$ on each n-dimensional rectangular element; the minimal finite element space for σ_{ij} would be span$\{1, x_i, x_j\}$ on each n-dimensional rectangular element. For the displacement (1.3), there is no derivative and the minimal finite element space would be the constant space span$\{1\}$. The spaces are displayed in the right diagram in Figure 1 and in Figure 2. Surprisingly, it is shown that these minimal finite element spaces can actually form a family of stable and convergent methods for (1.1). However, the analysis herein has to overcome the difficulty to prove the discrete inf-sup condition, one key ingredient for the stability analysis of the mixed finite element method [12], and the difficulty related to nonconformity of the discrete spaces for the stresses. For both the elasticity problem and the Poisson problem, the stability analysis of mixed finite element methods in literature is established by special commuting properties of canonical interpolation operators defined by degrees of freedom of discrete stress spaces, see, for instance, [1, 3, 4, 8] and [12]. To overcome the first difficulty, a new macro-element technique is proposed to prove a Fortin Lemma for mixed methods under consideration. Note that the macro-element technique is widely used to analyze the stability of mixed methods for the Stokes problem, see [12] and references therein. However, it is not used to the elasticity problem before. For the pure displacement

problem, an explicit constructive proof is also given for the discrete inf-sup condition. In order to deal with the second difficulty, a superconvergence property of the consistency error is proved. The mathematical *elegance and beauty* of this family of minimal elements is gestated within, besides the *perfect matching*, the independence of the spatial dimension n. In n dimension, the constructive proof of the discrete inf-sup condition can be divided into n steps of that for the 1D Raviart-Thomas element, and the consistency error can be decomposed as n two-dimensional consistency errors (For 1D, there is no consistency error.)

The superiority of the family of elements over the existing elements in the literature is its simplicity and high accuracy. In fact, a family of 2D rectangular, conforming elements, of which the lowest order has 45 stress and 12 displacement degrees of freedom per element, is proposed in [3]. A nonconforming mixed finite element based on rectangular grids is proposed with 19 stress and 6 displacement degrees of freedom on each element in [30]. Later on, a simplified mixed finite element on 2D rectangular grids is constructed with 13 stress and 4 displacement degrees of freedom on each rectangle independently in [21, 31], see the left diagram in Figure 1, which is the simplest rectangular element of first order in 2D in the literature so far. Doubtless, the 2D element with 7 stress and 2 displacement degrees of freedom on each rectangle of this paper is the simplest rectangular element, see the right diagram in Figure 1. Due to a perfect matching (for symmetry constraint), the new element has much less degrees of freedom (dof) but a higher order of approximation property, compared to previous elements [21, 30, 31]. This is confirmed by numerical results. In 3D, the new element has only 15 stress plus 3 displacement dof on each element, much simpler than the first order element, with 54 plus 12 dof per element, of [23]. Notice that the element of [23] is previously the simplest rectangular element in 3D.

The rest of the paper is organized as follows. The minimal element in 2D is introduced in Section 2. The well-posedness of the finite element problem, i.e. the discrete coerciveness and the discrete inf-sup condition, is proved in Section 3 for the pure displacement problem. The optimal order convergence is shown in Section 4. The element is extended to any space-dimension in Section 5. In Section 6, the stability of the minimal element is shown for the pure traction problem. Numerical results in 2D and 3D, including that for a pure traction problem, are provided in Section 7, which show a superconvergence of the minimal elements herein.

2. A minimal element in 2D

The 2D element is presented separately in this section for fixing the main idea while the whole family will be developed in Section 5. Also for simplicity we consider a pure displacement problem first. The analysis for other boundary value problems will be given in Section 6.

Consider a pure displacement problem (and a pure traction problem in Section 6):

$$\operatorname{div}(A^{-1}\epsilon(u)) = f \quad \text{in } \Omega, \tag{2.1a}$$

$$u = 0 \quad \text{on } \Gamma = \partial\Omega, \tag{2.1b}$$

The domain is assumed to be a rectangle (it is straightforward that results can be extended to domains which can be covered by rectangles), which is subdivided by a family of rectangular grids $\mathcal{T}_h$ (with grid size h).

The set of all edges in $\mathcal{T}_h$ is denoted by $\mathcal{E}_h$, which is divided into two sets, the set $\mathcal{E}_{h,H}$ of horizontal edges and the set $\mathcal{E}_{h,V}$ of vertical edges. Given any edge $e \in \mathcal{E}_h$, one fixed unit normal vector n with components (n_1, n_2) is assigned. For each $K \in \mathcal{T}_h$, define the affine invertible transformation

$$F_K : \qquad \hat{K} \to K,$$
$$\begin{pmatrix} \hat{x} \\ \hat{y} \end{pmatrix} \to \begin{pmatrix} x \\ y \end{pmatrix} = \begin{pmatrix} \frac{h_{x,K}}{2}\hat{x} + x_{0,K} \\ \frac{h_{y,K}}{2}\hat{y} + y_{0,K} \end{pmatrix},$$

with the center $(x_{0,K}, y_{0,K})$ of K, the horizontal length $h_{x,K}$, and the vertical length $h_{y,K}$, and the reference element $\hat{K} = [-1, 1]^2$.

On each element $K \in \mathcal{T}_h$, a constant finite element space for the displacement is defined by

$$V_K = \mathcal{P}_0(K, \mathbb{R}^2) = \Big\{ \begin{pmatrix} v_1 \\ v_2 \end{pmatrix} \mid v_1, v_2 \in P_0(K) \Big\}; \tag{2.2}$$

while the symmetric linear finite element space for the stress is defined by

$$\Sigma_K = \Big\{ \sigma \in \begin{pmatrix} P_{1,1}(K) & \mathcal{P}_1(K) \\ \mathcal{P}_1(K) & P_{1,2}(K) \end{pmatrix}_{\mathbb{S}} \Big\}, \tag{2.3}$$

where subscript $\mathbb{S}$ indicates a symmetric matrix stress, and

$$\begin{aligned} P_{1,1}(K) &= \mathrm{span}\{1, x\}, \\ \mathcal{P}_1(K) &= \mathrm{span}\{1, x, y\}, \\ P_{1,2}(K) &= \mathrm{span}\{1, y\}. \end{aligned}$$

The dimension of the space V_K is 2, and that of Σ_K is 7. The nodal degrees of freedom for (v_1, v_2), σ_{11}, and σ_{22}, are

- the moment of degree 0 on K for v_1 and v_2;
- the moments of degree 0 on two vertical edges of K for σ_{11};
- the moments of degree 0 on two horizontal edges of K for σ_{22};

The nodal degrees of freedom for σ_{12} will be studied as follows. Locally $\mathcal{P}_1(K)$ is the space of linear polynomials. Globally, let W_h be the P_1-nonconforming space on $\mathcal{T}_h$, which is first introduced in [25] as a nonconforming approximation space to $H^1(\Omega)$ on the quadrilateral mesh; see also [20]. To be exact, W_h is the space of piecewise linear polynomials, which are continuous at all mid-edge points of triangulation $\mathcal{T}_h$. W_h is the finite element space approximating function σ_{12}.

The global spaces Σ_h and V_h are defined by

$$\begin{aligned} \Sigma_h = \{\ \sigma = \begin{pmatrix} \sigma_{11} & \sigma_{12} \\ \sigma_{12} & \sigma_{22} \end{pmatrix} \in L^2(\Omega, \mathbb{S}) \mid \sigma|_K \in \Sigma_K \ \text{ for all } K \in \mathcal{T}_h, \\ \sigma_{11} \text{ is continuous on all vertical interior edges,} \\ \sigma_{22} \text{ is continuous on all horizontal interior edges,} \\ \sigma_{12} \text{ is continuous at all mid-points of interior edges } \}, \end{aligned} \tag{2.4}$$

$$V_h = \{ v \in L^2(\Omega, \mathbb{R}^2) \mid v|_K \in V(K) \ \text{ for all } K \in \mathcal{T}_h \}. \tag{2.5}$$

Since σ_{11} is continuous on all vertical interior edges, the derivative $\partial_x \sigma_{11}$ is well-defined in $L^2(\Omega)$. However, σ_{12} is not continuous on Ω so that $\partial_x \sigma_{12}$ and $\partial_y \sigma_{12}$ are not in $L^2(\Omega)$. Therefore the discrete stress space Σ_h is a nonconforming approximation to $H(\mathrm{div}, \Omega, \mathbb{S})$. So the discrete divergence operator div_h is defined elementwise with respect to $\mathcal{T}_h$,

$$\mathrm{div}_h\, \tau|_K = \mathrm{div}(\tau|_K) \quad \forall \tau \in \Sigma_h.$$

The mixed variational form for (2.1a) is (1.1). The mixed finite element approximation of Problem (1.1) reads: Find $(\sigma_h,\ u_h) \in \Sigma_h \times V_h$ such that

$$\begin{cases} (A\sigma_h, \tau) + (\mathrm{div}_h \tau, u_h) = 0 & \forall \tau \in \Sigma_h, \\ \qquad\qquad (\mathrm{div}_h\, \sigma_h, v) = (f, v) & \forall v \in V_h. \end{cases} \tag{2.6}$$

It follows from the definition of Σ_K that $\mathrm{div}_h\, \tau_h$ are piecewise constant for any $\tau_h \in \Sigma_h$, which leads to

$$\mathrm{div}_h\, \Sigma_h \subset V_h.$$

This, in turn, leads to a strong discrete divergence-free space:

$$\begin{aligned} Z_h &= \{ \tau_h \in \Sigma_h \mid (\mathrm{div}_h\, \tau_h, v) = 0 \quad \forall v \in V_h \} \\ &= \{ \tau_h \in \Sigma_h \mid \ \mathrm{div}_h\, \tau_h = 0 \text{ pointwise } \}. \end{aligned} \tag{2.7}$$

For the analysis, define the following broken norm:

$$\|\tau\|_{H(\mathrm{div}_h)} = (\|\tau\|_0^2 + \|\mathrm{div}_h \tau\|_0^2)^{1/2} \quad \forall \tau \in \Sigma_h. \tag{2.8}$$

The rest of this section is devoted to an alternative definition to W_h, the space for σ_{12} in Σ_h. The dimension of the space $\mathcal{P}_1(K)$ is three, less than the number of edges or vertexes of element K. The discrete shear stress σ_{12} is still defined by four vertex-value functionals, which are not linearly independent though. A constraint can be posed on those four functionals if one defines a functional set $\mathcal{N}$ on $\mathcal{P}_1(K)$, cf. [25, Lemma 2.1].

Here the idea from [20] of a frame for $\mathcal{P}_1(K)$ will be used. To this end, define the frame for the space $\mathcal{P}_1(\hat{K}) = \mathrm{span}\{1, \hat{x}, \hat{y}\}$ by

$$\phi_{-1,-1} = \frac{1-\hat{x}-\hat{y}}{4}, \qquad \phi_{1,-1} = \frac{1+\hat{x}-\hat{y}}{4},$$
$$\phi_{1,1} = \frac{1+\hat{x}+\hat{y}}{4}, \qquad \phi_{-1,1} = \frac{1-\hat{x}+\hat{y}}{4}.$$

This frame is depicted in Figure 3.

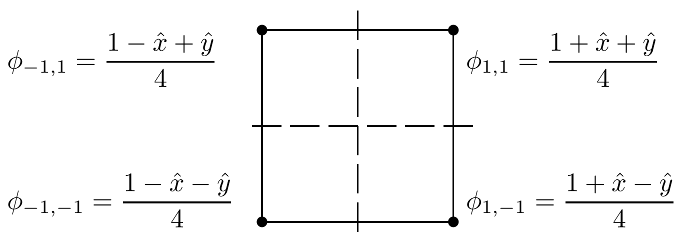

FIGURE 3. Four nodal (frame/not basis) functions of W_h on $\hat{K}$.

An interpolation operator Π_{12}, from $H^2(\Omega)$ (i.e., some continuous functions) to W_h is needed. The interpolation on $\hat{K}$ is defined as

$$\begin{aligned}\hat{\Pi}_{12}\hat{\sigma}_{12} = {} & \hat{\sigma}_{12}(\hat{x}_{1,\hat{K}}, \hat{y}_{1,\hat{K}})\phi_{-1,-1} + \hat{\sigma}_{12}(\hat{x}_{2,\hat{K}}, \hat{y}_{2,\hat{K}})\phi_{1,-1} \\ & + \hat{\sigma}_{12}(\hat{x}_{3,\hat{K}}, \hat{y}_{3,\hat{K}})\phi_{1,1} + \hat{\sigma}_{12}(\hat{x}_{4,\hat{K}}, \hat{y}_{4,\hat{K}})\phi_{-1,1},\end{aligned}$$

where the four vertexes are numbered counterclock wise,

$$\begin{aligned}(\hat{x}_{1,\hat{K}}, \hat{y}_{1,\hat{K}}) &= (-1,-1), \\ (\hat{x}_{2,\hat{K}}, \hat{y}_{2,\hat{K}}) &= (1,-1), \\ (\hat{x}_{3,\hat{K}}, \hat{y}_{3,\hat{K}}) &= (1,1), \\ (\hat{x}_{4,\hat{K}}, \hat{y}_{4,\hat{K}}) &= (-1,1).\end{aligned}$$

In the same fashion, the interpolation Π_{12} is defined on all $K \in \mathcal{T}_h$ by

$$\begin{aligned}\Pi_{12}\sigma_{12}(x,y) = {} & \sigma_{12}(x_{1,K}, y_{1,K})\phi_{-1,-1}(F_K^{-1}(x,y)) \\ & + \sigma_{12}(x_{2,K}, y_{2,K})\phi_{1,-1}(F_K^{-1}(x,y)) \\ & + \sigma_{12}(x_{3,K}, y_{3,K})\phi_{1,1}(F_K^{-1}(x,y)) \\ & + \sigma_{12}(x_{4,K}, y_{4,K})\phi_{-1,1}(F_K^{-1}(x,y)),\end{aligned} \tag{2.9}$$

where $(x,y) \in K$, and $(x_{i,K}, y_{i,K})$ are the four vertexes of K. As $\phi_{-1,-1}(0,-1) = \phi_{1,-1}(0,-1) = 1/2$, it follows that

$$\Pi_{12}\sigma_{12}|_{e_\pm}(e_m) = \frac{1}{2}\left(\sigma_{12}(e_1) + \sigma_{12}(e_2)\right),$$

where e_+ and e_- are two sides of an edge $e \in \mathcal{E}_h$, e_m is the mid-point of e, and e_1 and e_2 are two endpoints of e. That is, $\Pi_{12}\sigma_{12}$ is continuous at all mid-points of edges. For a vertex in $\mathcal{T}_h$,

$$c_{i,j} = (ih, jh), \quad 0 \le i, j \le N, \ N = 1/h,$$

it may be shared by one, or two, or four elements $K \in \mathcal{T}_h$. The combination of the frame functions at the vertex $c_{i,j}$ forms one global frame function $\phi_{i,j}$. For example, at vertex $c_{0,1}$, as it is shared by two elements, $K_{1,1} = [0, h] \times [0, h]$ and $K_{1,2} = [0, h] \times [h, 2h]$,

$$\psi_{0,1} = \begin{cases} \phi_{-1,1}(\frac{2}{h}(x - \frac{h}{2}), \frac{2}{h}(y - \frac{h}{2})) & (x, y) \in K_{1,1}, \\ \phi_{-1,-1}(\frac{2}{h}(x - \frac{h}{2}), \frac{2}{h}(y - \frac{3h}{2})) & (x, y) \in K_{1,2}, \\ 0 & \text{elsewhere on } \ \Omega. \end{cases}$$

Note that $\psi_{i,j}$ is not continuous at $c_{i,j}$. Thus, the finite element space for σ_{12} in (2.4) is

$$W_h = \{s \in L^2(\Omega) \ \mid \ s = \sum_{i,j=0}^{N} p_{ij}\psi_{i,j}\}. \tag{2.10}$$

3. Well-posedness of the discrete problem in 2D

This section considers the well-posedness of the discrete problem (2.6), which needs the following two conditions.

(1) K-ellipticity. There exists a constant $C > 0$, independent of the meshsize h such that

$$(A\tau, \tau) \ge C\|\tau\|^2_{H(\mathrm{div}_h)} \quad \forall \tau \in Z_h, \tag{3.1}$$

where Z_h is the divergence-free space defined in (2.7).

(2) Discrete B-B condition. There exists a positive constant $C > 0$ independent of the meshsize h, such that

$$\inf_{v \in V_h} \sup_{\tau \in \Sigma_h} \frac{(\mathrm{div}_h \tau, v_h)}{\|\tau\|_{H(\mathrm{div}_h)}\|v\|_0} \ge C. \tag{3.2}$$

Theorem 3.1. *For the discrete problem (2.6), the K-ellipticity* (3.1) *and the discrete B-B condition* (3.2) *hold uniformly. Consequently, the discrete mixed problem* (2.6) *has a unique solution* $(\sigma_h, \ u_h) \in \Sigma_h \times V_h$.

Proof. It follows from (2.7) that for all $\tau \in Z_h$, $\mathrm{div}_h \tau = 0$. Thus $\| \mathrm{div}_h \tau\|_0 = 0$ and $\|\tau\|_{H(\mathrm{div}_h)} = \|\tau\|_0$. Since the operator A is symmetric and positive definite, the K-ellipticity of the bilinear form $(A\tau, \tau)$ follows.

It remains to show the discrete B-B condition (3.2). Since the usual technique based on canonical interpolations operators for discrete stress spaces [4, 8] is inapplicable here, a constructive proof is adopted. For convenience, suppose that the domain Ω is a unit square $[0, 1]^2$ which is triangulated evenly into N^2 elements, $\{K_{ij}\}$. For any $v \in V_h$, it can be decomposed as a sum,

$$v_h = \sum_{i=1}^{N}\sum_{j=1}^{N} V_{ij}\varphi_{ij}(x, y), \tag{3.3}$$

where $\varphi_{ij}(x)$ is the characteristic function on the element K_{ij}, and $V_{ij} = (V_{1,ij}, V_{2,ij}) = (v_h|_{K_{ij}})$. A discrete stress function $\tau_h \in \Sigma_h$ will be constructed with

$$\mathrm{div}_h \, \tau_h = v_h \text{ and } \|\tau_h\|_{H(\mathrm{div}_h)} \le C\|v_h\|_0.$$

The construction of τ_h is motivated by a simple proof of the inf-sup condition of the 1D Raviart-Thomas element for the 1D Poisson problem. The shear stress τ_{12} can be taken zero, i.e., $\tau_{12} \equiv 0$; the normal stress τ_{11} (resp. τ_{22}) of τ_h can be constructed so that it is independent of the second (resp. first) component of

v_h. In addition, τ_{11} (resp. τ_{22}) can be a continuous piecewise linear function of the variable x (resp. y) and a piecewise constant function of y (resp. x). Therefore, they are of form

$$\tau_{11}(x,y) = h\sum_{m=1}^{i-1} V_{1,mj} + V_{1,ij}(x - x_{i-1}), \tag{3.4}$$

$$\tau_{22}(x,y) = h\sum_{k=1}^{j-1} V_{2,ik} + V_{2,ij}(y - y_{j-1}), \tag{3.5}$$

for $x_{i-1} \le x < x_i$ and $y_{j-1} \le y < y_j$ ((x_i, y_j) is the upper-right corner vertex of square K_{ij}.) Thus, define

$$\tau_h = \begin{pmatrix} \tau_{11} & 0 \\ 0 & \tau_{22} \end{pmatrix} \in \Sigma_h.$$

By this construction, $\partial_x \tau_{11} = (v_h)_1$ and $\partial_y \tau_{22} = (v_h)_2$. This gives

$$\mathrm{div}_h \tau_h = v_h. \tag{3.6}$$

An elementary calculation gives

$$\begin{aligned} \|v_h\|_0^2 &= \sum_{i,j=1}^{N} \|V_{ij}\varphi_{ij}\|_{0,K_{ij}}^2 = \sum_{i,j=1}^{N} \int_{K_{ij}} |V_{ij}\varphi_{ij}|^2 \, dxdy \\ &= \sum_{i,j=1}^{N} ((V_{1,ij})^2 + (V_{2,ij})^2)h^2. \end{aligned}$$

By the Schwarz inequality,

$$\begin{aligned} \|\tau_{11}\|_0^2 &= \sum_{i,j=1}^{N} \int_{K_{ij}} \left(h\sum_{m=1}^{i-1} V_{1,mj} + V_{1,ij}(x - x_{i-1}) \right)^2 dxdy \\ &\le \sum_{i,j=1}^{N} \int_{K_{ij}} \left(h^2 \sum_{m=1}^{i-1} (V_{1,mj}) + (V_{1,ij})(x - x_{i-1})^2 \right) \cdot i \, dxdy. \end{aligned}$$

Further, since $N = 1/h$ and $\int_{K_{ij}} = h^2$,

$$\begin{aligned} \|\tau_{11}\|_0^2 &\le \sum_{i,j=1}^{N} \left(h^2 \sum_{m=1}^{i} (V_{1,mj})^2 \right) \cdot Nh^2 \le \sum_{j=1}^{N} \left(h^2 \sum_{m=1}^{N} (V_{1,mj})^2 \right) \cdot N^2h^2 \\ &= h^2 \sum_{i,j=1}^{N} (V_{1,ij})^2. \end{aligned}$$

A similar argument leads to

$$\|\tau_{22}\|_0^2 \le h^2 \sum_{i,j=1}^{N} (V_{2,ij})^2.$$

The combination of the aforementioned two identities and two inequalities yields

$$\begin{aligned} \|\tau_h\|_{H(\mathrm{div}_h)}^2 &= \|\tau_h\|_0^2 + \|\mathrm{div}_h \tau_h\|_0^2 \\ &= \|\tau_{11}\|_0^2 + \|\tau_{22}\|_0^2 + \|v_h\|_0^2 \le 2\|v_h\|_0^2. \end{aligned}$$

Hence, for any $v_h \in V_h$, the B-B condition (3.2) holds with $C = 1/\sqrt{2}$:

$$\inf_{v_h \in V_h} \sup_{\tau \in \Sigma_h} \frac{(\mathrm{div}_h \tau, \ v_h)}{\|\tau\|_{H(\mathrm{div}_h)} \|v_h\|_0} \ge \inf_{v_h \in V_h} \frac{\|v_h\|_0^2}{\sqrt{2}\|v_h\|_0^2} = \frac{1}{\sqrt{2}}.$$

This completes the proof. ∎

4. Error analysis in 2D

The section is devoted to the error estimate stated in Theorem 4.3, which is based on the approximation error estimate of Theorem 4.1 and the consistency error estimate of Theorem 4.2.

In order to analyze the approximation error, for any $\tau \in H(\mathrm{div}, \Omega, \mathbb{S}) \cap H^2(\Omega, \mathbb{S})$, define an interpolation

$$\Pi_h \sigma = \begin{pmatrix} \Pi_{11}\sigma_{11} & \Pi_{12}\sigma_{12} \\ \Pi_{12}\sigma_{12} & \Pi_{22}\sigma_{22} \end{pmatrix} \in \Sigma_h, \tag{4.1}$$

where Π_{11} and Π_{22} are standard, satisfying, respectively,

$$\int_e \Pi_{11}\sigma_{11} ds = \int_e \sigma_{11} ds \text{ for any vertical edge } e \in \mathcal{E}_h, \tag{4.2}$$

$$\int_e \Pi_{22}\sigma_{22} ds = \int_e \sigma_{22} ds \text{ for any horizontal edge } e \in \mathcal{E}_h. \tag{4.3}$$

Π_{12} is the interpolation operator defined in (2.9), from the space $H^2(\Omega)$ to W_h. It is shown by Park and Sheen [25] that

$$|v - \Pi_{12} v|_{m,K} \leq C h^{2-m} |v|_{2,K}, \ m = 0, 1, \quad K \in \mathcal{T}_h. \tag{4.4}$$

Theorem 4.1. *For any $\sigma \in H^2(\Omega, \mathbb{S})$, it holds that*

$$\|\sigma - \Pi_h \sigma\|_0 \leq C h \|\sigma\|_1,$$
$$\|\mathrm{div_h}(\sigma - \Pi_h \sigma)\|_0 \leq C h \|\sigma\|_2.$$

Proof. By the scaling argument and the standard approximation theory, the following two estimates will be proved

$$|\sigma_{11} - \Pi_{11}\sigma_{11}|_{0,K} \leq C h |\sigma_{11}|_{1,K} \quad \forall K \in \mathcal{T}_h, \tag{4.5}$$

$$|\frac{\partial}{\partial x}(\sigma_{11} - \Pi_{11}\sigma_{11})|_{0,K} \leq C h |\frac{\partial \sigma_{11}}{\partial x}|_{1,K} \quad \forall K \in \mathcal{T}_h. \tag{4.6}$$

For any element $K \in \mathcal{T}_h$, by (4.2) (i.e., the interpolation (4.2) is equivalent to a mid-point interpolation),

$$\begin{aligned} \|\sigma_{11} - \Pi_{11}\sigma_{11}\|_{0,K}^2 &= \frac{h_x h_y}{4} \int_{\hat{K}} |\hat{\sigma}_{11} - \hat{\Pi}_{11}\hat{\sigma}_{11}|^2 d\hat{x} d\hat{y} \\ &\leq C h^2 |\hat{\sigma}_{11}|_{1,\hat{K}}^2 \leq C h^2 |\sigma_{11}|_{1,K}^2. \end{aligned}$$

This is (4.5). By the reference mapping,

$$\begin{aligned} \left\| \frac{\partial}{\partial x}(\sigma_{11} - \Pi_{11}\sigma_{11}) \right\|_{0,K}^2 &= \frac{h_y}{h_x} \int_{\hat{K}} |\frac{\partial}{\partial \hat{x}}(\hat{\sigma}_{11} - \hat{\Pi}_{11}\hat{\sigma}_{11})|^2 \, d\hat{x} d\hat{y} \\ &\leq C \int_{\hat{K}} |\frac{\partial}{\partial \hat{x}}\hat{\sigma}_{11} - \frac{\partial}{\partial \hat{x}}\hat{\Pi}_{11}\hat{\sigma}_{11}|^2 d\hat{x} d\hat{y}. \end{aligned} \tag{4.7}$$

Now

$$\begin{aligned} \int_{\hat{K}} \frac{\partial}{\partial \hat{x}} \hat{\Pi}_{11}\hat{\sigma}_{11} d\hat{x} d\hat{y} &= \int_{-1}^{1} \{(\hat{\Pi}_{11}\hat{\sigma}_{11})(1, \hat{y}) - (\hat{\Pi}_{11}\hat{\sigma}_{11})(-1, \hat{y})\} d\hat{y} \\ &= \int_{-1}^{1} \{\hat{\sigma}_{11}(1, \hat{y}) - \hat{\sigma}_{11}(-1, \hat{y})\} d\hat{y} \\ &= \int_{\hat{K}} \frac{\partial \hat{\sigma}_{11}}{\partial \hat{x}} \, d\hat{x} d\hat{y}, \end{aligned}$$

This means $\frac{\partial}{\partial\hat{x}}(\hat{\Pi}_{11}\hat{\sigma}_{11}) = P_{0,\hat{K}}(\frac{\partial\hat{\sigma}_{11}}{\partial\hat{x}})$, where $P_{0,\hat{K}}$ is the projection operator onto the constant space on element $\hat{K}$. A substitution of it into (4.7) leads to

$$\begin{aligned}\left\|\frac{\partial}{\partial x}(\sigma_{11} - \Pi_{11}\sigma_{11})\right\|_{0,K}^2 &\le C\left\|\frac{\partial\hat{\sigma}_{11}}{\partial\hat{x}} - P_{0,\hat{K}}(\frac{\partial\hat{\sigma}_{11}}{\partial\hat{x}})\right\|_{0,\hat{K}}^2\\ &\le C\inf_{c\in\mathbb{R}}\left\|(\frac{\partial\hat{\sigma}_{11}}{\partial\hat{x}} - c)\right\|_{0,\hat{K}}^2.\end{aligned}$$

By the Bramble-Hilbert Lemma,

$$\left\|\frac{\partial}{\partial x}(\sigma_{11} - \Pi_{11}\sigma_{11})\right\|_{0,K}^2 \le C\left|\frac{\partial\hat{\sigma}_{11}}{\partial\hat{x}}\right|_{1,\hat{K}}^2 \le Ch^2\left|\frac{\partial\sigma_{11}}{\partial x}\right|_{1,K}^2.$$

This is (4.6).

A similar argument yields

$$\|\sigma_{22} - \Pi_{22}\sigma_{22}\|_{0,K} \le Ch|\sigma_{22}|_{1,K} \quad \forall K\in\mathcal{T}_h, \tag{4.8}$$

$$\left\|\frac{\partial}{\partial y}(\sigma_{22} - \Pi_{22}\sigma_{22})\right\|_{0,K} \le Ch\left|\frac{\partial\sigma_{22}}{\partial y}\right|_{1,K} \quad \forall K\in\mathcal{T}_h. \tag{4.9}$$

Noting that the L^2 norm on Σ is

$$\|\sigma\|_{0,K}^2 = \|\sigma_{11}\|_{0,K}^2 + 2\|\sigma_{12}\|_{0,K}^2 + \|\sigma_{22}\|_{0,K}^2,$$

A combination of the estimates (4.5), (4.6), (4.8), (4.9) and (4.4), completes the proof. ∎

Theorem 4.2. *Assume that (σ, u) be the solution to the problem (1.1) with $u \in H_0^1(\Omega,\mathbb{R}^2)\cap H^2(\Omega,\mathbb{R}^2)$. Then,*

$$\sup_{\tau_h\in\Sigma_h}\frac{(A\sigma,\tau_h) + (\mathrm{div}_h\tau_h, u)}{\|\tau_h\|_{H(\mathrm{div}_h)}} \le Ch|u|_2. \tag{4.10}$$

Proof. It follows from the first equation of (1.1) that $A\sigma = \frac{1}{2}(\nabla u + \nabla u^T)$ for the exact solution $u \in H_0^1(\Omega,\ \mathbb{R}^2)$. An elementwise integration by parts gives

$$(\epsilon(u),\tau_h) = -(\mathrm{div}_h\tau_h, u) + \sum_{K\in\mathcal{T}_h}\int_{\partial K}\tau_h n\cdot u ds \quad \forall\tau_h\in\Sigma_h,$$

which implies

$$(A\sigma,\tau_h) + (\mathrm{div}_h\tau_h, u) = \sum_{K\in\mathcal{T}_h}\int_{\partial K}\tau_h n\cdot u ds. \tag{4.11}$$

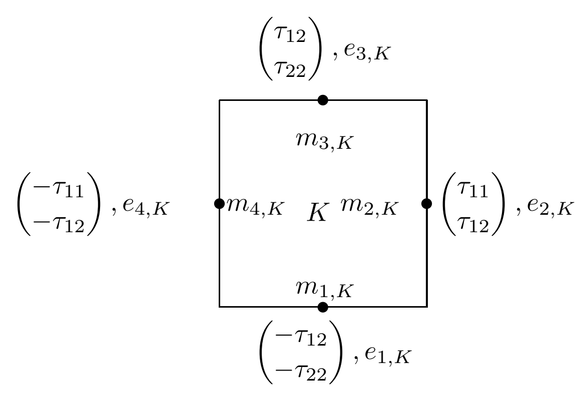

FIGURE 4. $\tau_h\cdot n$ on the four edges of element K, cf. (4.12).

Let $\tau_h|_K = \begin{pmatrix}\tau_{11} & \tau_{12}\\ \tau_{21} & \tau_{22}\end{pmatrix}$, cf. Figure 4. Since τ_{11} is continuous in the x-direction and τ_{22} is continuous in the y-direction, there is a cancellation for these two components on the inter-element boundary. Since $u \in H^2(\Omega,\mathbb{R}^2)\cap H_0^1(\Omega,\mathbb{R}^2)$,

$$\begin{aligned}(4.12)\qquad &\sum_{K\in\mathcal{T}_h}\int_{\partial K}\tau_h\cdot n u ds\\ &= \sum_{K\in\mathcal{T}_h}\Big[(\int_{e_{2,K}}-\int_{e_{4,K}})\tau_{12}u_2 ds + (\int_{e_{1,K}}-\int_{e_{3,K}})\tau_{12}u_1 ds\Big].\end{aligned}$$

For any $v\in H^1(K)$, define the L^2-projection operator J_e on an edge e by

$$J_e v = \frac{1}{|e|}\int_e v ds.$$

Because τ_{12} is continuous at the mid-point of all edges, it follows that, including boundary edges where $u_i = 0$, on the horizontal edges $\mathcal{E}_{h,H}$,

$$\begin{aligned}\sum_{K\in\mathcal{T}_h}(\int_{e_{1,K}}-\int_{e_{3,K}})\tau_{12}u_1 ds &= \sum_{e\in\mathcal{E}_{h,H}}\int_e(\tau_{12}|_{e_+}-\tau_{12}|_{e_-})u_1 ds\\ &= \sum_{e\in\mathcal{E}_{h,H}}\int_e(\tau_{12}|_{e_+}-\tau_{12}|_{e_-})(u_1 - J_e u_1)ds.\end{aligned}$$

After inserting a same constant $J_K\tau_{12} = \int_K \tau_{12}dxdy/|K|$ into the two integrals on two horizontal edges of one element K, the sum can be rewritten as

$$\begin{aligned}(4.13)\qquad &\sum_{K\in\mathcal{T}_h}(\int_{e_{1,K}}-\int_{e_{3,K}})\tau_{12}u_1 ds\\ &= \sum_{K\in\mathcal{T}_h}\int_{e_{1,K}}\tau_{12}(u_1 - J_{e_{1,K}}u_1)ds - \int_{e_{3,K}}\tau_{12}(u_1 - J_{e_{3,K}}u_1)ds\\ &= \sum_{K\in\mathcal{T}_h}\int_{e_{1,K}}(\tau_{12}-J_K\tau_{12})(u_1 - J_{e_{1,K}}u_1)ds\\ &\qquad - \int_{e_{3,K}}(\tau_{12}-J_K\tau_{12})(u_1 - J_{e_{3,K}}u_1)ds.\end{aligned}$$

There is some superconvergence property for the two terms in (4.13) if they are considered together. In fact, on the reference element $\hat{K}$, $\hat{\tau}_{12}(\hat{x},\pm 1) = \hat{\tau}_{12}(0,0) + \hat{x}\partial_{\hat{x}}\hat{\tau}_{12}(0,0) \pm \partial_{\hat{y}}\hat{\tau}_{12}(0,0)$, and $J_{\hat{K}}\hat{\tau}_{12} = \hat{\tau}_{12}(0,0)$. The property of J_e gives

$$\begin{aligned}&\frac{1}{2}\int_{-1}^{1}(\hat{\tau}_{12}-J_{\hat{K}}\hat{\tau}_{12})\Big[(\hat{u}_1 - \hat{J}_{\hat{e}_1}\hat{u}_1)(\hat{x},-1) - (\hat{u}_1 - \hat{J}_{\hat{e}_3}\hat{u}_1)(\hat{x},1)\Big]d\hat{x}\\ &= -\frac{1}{2}\int_{-1}^{1}\hat{x}\frac{\partial}{\partial\hat{x}}\hat{\tau}_{12}\Big[\int_{-1}^{1}\frac{\partial}{\partial\hat{y}}\hat{u}_1 d\hat{y} - \frac{1}{2}\int_{-1}^{1}(\hat{u}(\hat{x},1)-\hat{u}(\hat{x},-1))d\hat{x}\Big]d\hat{x}\\ &= -\frac{1}{2}\int_{-1}^{1}\hat{x}\frac{\partial}{\partial\hat{x}}\hat{\tau}_{12}\Big[\int_{-1}^{1}\frac{\partial}{\partial\hat{y}}\hat{u}_1 d\hat{y} - \frac{1}{2}\int_{-1}^{1}(\int_{-1}^{1}\frac{\partial}{\partial\hat{y}}\hat{u}(\hat{x},\hat{y})d\hat{y})d\hat{x}\Big]d\hat{x}\\ &= -\frac{1}{4}\int_{-1}^{1}\hat{x}\frac{\partial}{\partial\hat{x}}\hat{\tau}_{12}\Big[\int_{-1}^{1}\int_{-1}^{1}(\frac{\partial}{\partial\hat{y}}\hat{u}_1(\hat{x},\hat{y}) - \frac{\partial}{\partial\hat{y}}\hat{u}(\hat{t},\hat{y}))d\hat{y}d\hat{t}\Big]d\hat{x}\\ &= -\frac{1}{4}\int_{-1}^{1}\hat{x}\frac{\partial}{\partial\hat{x}}\hat{\tau}_{12}\Big[\int_{-1}^{1}\int_{-1}^{1}\int_{\hat{t}}^{\hat{x}}\frac{\partial^2}{\partial\hat{x}\partial\hat{y}}\hat{u}_1(\hat{s},\hat{y})d\hat{s}d\hat{y}d\hat{t}\Big]d\hat{x}.\end{aligned}$$

By the Schwarz inequality and (4.13),

$$
\begin{aligned}
&\left|\sum_{K\in\mathcal{T}_h}\Big(\int_{e_{1,K}}-\int_{e_{3,K}}\Big)\tau_{12}u_1ds\right|^2\\
&=\frac{h^2}{2^2}\left|\sum_{K\in\mathcal{T}_h}\int_{-1}^{1}\frac{\partial}{\partial\hat{x}}\hat{\tau}_{12}\hat{x}\Big[\int_{-1}^{1}\int_{-1}^{1}\int_{\hat{t}}^{\hat{x}}\frac{\partial^2}{\partial\hat{x}\partial\hat{y}}\hat{u}_1(\hat{s},\hat{y})d\hat{s}d\hat{y}d\hat{t}\Big]d\hat{x}\right|^2\\
&\le Ch^2\left(\sum_{K\in\mathcal{T}_h}\left\|\frac{\partial}{\partial\hat{x}}\hat{\tau}_{12}\right\|_{0,\hat{K}}^2\right)\left(\sum_{K\in\mathcal{T}_h}\left\|\frac{\partial^2}{\partial\hat{x}\partial\hat{y}}\hat{u}_1\right\|_{0,\hat{K}}^2\right)\\
&=Ch^2\left(\left\|\frac{\partial}{\partial x}\tau_{12}\right\|_0^2\frac{h^2}{2^2}\left\|\frac{\partial^2}{\partial x\partial y}u_1\right\|_0^2\right)\\
&\le Ch^4|\tau_{12}|_{1,h}^2|u_1|_2^2.
\end{aligned}
$$

Here $|\cdot|_{1,h}$ is the elementwise semi-H^1 norm. A similar argument bounds the other term in (4.12) by

$$
\left|\sum_{K\in\mathcal{T}_h}\Big(\int_{e_{2,K}}-\int_{e_{4,K}}\Big)\tau_{12}u_2ds\right|\le Ch^2|\tau_{12}|_{1,h}|u_2|_2.
$$

A combination of these two estimates with (4.11) implies

$$
|(A\sigma,\tau_h)+(\mathrm{div}_h\tau_h,u)|\le Ch^2|u|_2|\tau_h|_{1,h}.
$$

By the inverse inequality,

$$
|(A\sigma,\tau_h)+(\mathrm{div}_h\tau_h,u)|\le Ch|u|_2\|\tau_h\|_0. \tag{4.14}
$$

∎

Theorem 4.3. *Let* $(\sigma,u)\in\Sigma\times V$ *be the exact solution of problem* (1.1) *and* $(\tau_h,u_h)\in\Sigma_h\times V_h$ *the finite element solution of* (2.6). *Then*

$$
\begin{aligned}
\|\sigma-\sigma_h\|_0&\le Ch(\|u\|_2+\|\sigma\|_2),\\
\|\mathrm{div}_h(\sigma-\sigma_h)\|_0&\le Ch(\|u\|_2+\|\sigma\|_2),\\
\|u-u_h\|_0&\le Ch(\|u\|_2+\|\sigma\|_2).
\end{aligned}
$$

Proof. Let

$$
Z_f=\{\tau\in\Sigma_h\mid(\mathrm{div}_h\tau,v)=(f,v)\quad\forall v\in V_h\}.
$$

The finite element solution σ_h is in Z_f. Thus, for any $\tau\in Z_f$, it holds $\sigma_h-\tau\in Z_h$, i.e.,

$$
\mathrm{div}_h(\sigma_h-\tau)=0.
$$

It follows from the K-ellipticity (cf. (3.1)) that, for all $\tau\in Z_f$,

$$
\begin{aligned}
C\|\sigma_h-\tau\|_0^2&\le(A(\sigma_h-\tau),\sigma_h-\tau)\\
&=(A(\sigma-\tau),\sigma_h-\tau)+(A(\sigma_h-\sigma),\sigma_h-\tau)\\
&=(A(\sigma-\tau),\sigma_h-\tau)-(A\sigma,\sigma_h-\tau)-(\mathrm{div}_h(\sigma_h-\tau),u_h)\\
&=(A(\sigma-\tau),\sigma_h-\tau)-(A\sigma,\sigma_h-\tau)\\
&=(A(\sigma-\tau),\sigma_h-\tau)-(A\sigma,\sigma_h-\tau)-(\mathrm{div}_h(\sigma_h-\tau),u).
\end{aligned}
$$

An application of the Schwarz inequality leads to

$$\begin{aligned}\|\sigma_h-\tau\|_{H(\mathrm{div}_h)}&=\|\sigma_h-\tau\|_0\\&\le C\|\sigma-\tau\|_{H(\mathrm{div}_h)}-\frac{(A\sigma,\sigma_h-\tau)+(\mathrm{div}_h(\sigma_h-\tau),u)}{C\|\sigma_h-\tau\|_{H(\mathrm{div}_h)}}\\&=C\|\sigma-\tau\|_{H(\mathrm{div}_h)}+\sup_{\tau_h\in\Sigma_h}\frac{(A\sigma,\tau_h)+(\mathrm{div}_h\tau_h,u)}{C\|\tau_h\|_{H(\mathrm{div}_h)}}.\end{aligned}$$

By the triangle inequality,

$$\|\sigma-\sigma_h\|_{H(\mathrm{div}_h)}\le C\{\inf_{\tau\in Z_f}\|\sigma-\tau\|_{H(\mathrm{div}_h)}+\sup_{\tau_h\in\Sigma_h}\frac{(A\sigma,\tau_h)+(\mathrm{div}_h\tau_h,u)}{\|\tau_h\|_{H(\mathrm{div}_h)}}\}. \tag{4.15}$$

For a given $\tau_h\in\Sigma_h$, the discrete B-B condition (3.2) ensures that the following problem has at least one solution $\gamma_h\in\Sigma_h$, cf. [12],

$$(\mathrm{div}_h\gamma_h,v_h)=(\mathrm{div}_h(\sigma-\tau_h),v_h)\quad\forall\ v_h\in V_h. \tag{4.16}$$

It follows from the B-B condition (3.2) that

$$\begin{aligned}\|\gamma_h\|_{H(\mathrm{div}_h)}&\le\frac{1}{C}\sup_{v_h\in V_h}\frac{(\mathrm{div}_h\gamma_h,\ v_h)}{\|v_h\|_0}=\frac{1}{C}\sup_{v_h\in V_h}\frac{(\mathrm{div}_h(\sigma-\tau_h,\ v_h)}{\|v_h\|_0}\\&\le\frac{1}{C}\|\mathrm{div}_h(\sigma-\tau_h)\|_0.\end{aligned}$$

The identity (4.16) asserts that $\gamma_h+\tau_h\in Z_f$. The choice $\tau=\gamma_h+\tau_h$ in (4.15) leads to

$$\begin{aligned}&\|\sigma-\sigma_h\|_{H(\mathrm{div}_h)}\\&\le C\{\|\sigma-\tau_h\|_{H(\mathrm{div}_h)}+\|\gamma\|_{H(\mathrm{div}_h)}+\sup_{\tau_h\in\Sigma_h}\frac{(A\sigma,\tau_h)+(\mathrm{div}_h\tau_h,u)}{\|\tau_h\|_{H(\mathrm{div}_h)}}\}\\&\le C\{\|\sigma-\tau_h\|_{H(\mathrm{div}_h)}+\sup_{\tau_h\in\Sigma_h}\frac{(A\sigma,\tau_h)+(\mathrm{div}_h\tau_h,u)}{\|\tau_h\|_{H(\mathrm{div}_h)}}\}.\end{aligned}$$

That is,

$$\|\sigma-\sigma_h\|_{H(\mathrm{div}_h)}\le C\{\inf_{\tau_h\in\Sigma_h}\|\sigma-\tau_h\|_{H(\mathrm{div}_h)}+\sup_{\tau\in\Sigma_h}\frac{(A\sigma,\tau)+(\mathrm{div}_h\tau,u)}{\|\tau\|_{H(\mathrm{div}_h)}}\}. \tag{4.17}$$

The first term on the right-hand side of (4.17) is the approximation error. The choice $\tau_h=\Pi_h\sigma$ with Theorem 4.1 gives its upper bound. The second term on the right-hand side of (4.17) is the usual consistency error for the nonconforming finite element method, which has already been bounded in Theorem 4.2. A combination of these two theorems implies

$$\begin{aligned}\|\sigma-\sigma_h\|_0&\le Ch(\|u\|_2+\|\sigma\|_2),\\\|\mathrm{div}_h(\sigma-\sigma_h)\|_0&\le Ch(\|u\|_2+\|\sigma\|_2).\end{aligned}$$

The rest of the proof is concerned with the estimation of $u-u_h$. In view of the discrete B-B Condition (3.2), it holds, for any $v \in V_h$,

$$
\begin{aligned}
& C\|u_h - v\|_0 \\
\le & \sup_{\tau\in\Sigma_h} \frac{(\mathrm{div}_h\tau, u_h - v)}{\|\tau\|_{H(\mathrm{div}_h)}} = \sup_{\tau\in\Sigma_h} \frac{(\mathrm{div}_h\tau, u_h - u + u - v)}{\|\tau\|_{H(\mathrm{div}_h)}} \\
\le & \sup_{\tau\in\Sigma_h} \frac{(\mathrm{div}_h\tau, u_h - u)}{\|\tau\|_{H(\mathrm{div}_h)}} + \|u-v\|_0 \\
= & \sup_{\tau\in\Sigma_h} \frac{(\mathrm{div}_h\tau, u_h) + (A\sigma,\tau) - (A\sigma,\tau) - (\mathrm{div}_h\tau, u)}{\|\tau\|_{H(\mathrm{div}_h)}} + \|u-v\|_0 \\
= & \sup_{\tau\in\Sigma_h} \frac{(A(\sigma-\sigma_h),\tau) - (A\sigma,\tau) - (\mathrm{div}_h\tau, u)}{\|\tau\|_{H(\mathrm{div}_h)}} + \|u-v\|_0 \\
\le & \sup_{\tau\in\Sigma_h} \frac{(A\sigma,\tau) + (\mathrm{div}_h\tau, u)}{\|\tau\|_{H(\mathrm{div}_h)}} + C(\|\sigma-\sigma_h\|_0 + \|u-v\|_0).
\end{aligned}
$$

By (4.14) and the error estimation of $\|\sigma-\sigma_h\|_0$, the triangle inequality plus $v = P_h u$ (P_h is the L^2 projection into piecewise constant spaces) yield

$$
\begin{aligned}
\|u-u_h\|_0 &\le \|u - P_h u\|_0 + \|P_h u - u_h\|_0 \\
&\le Ch|u|_2 + C(\|\sigma-\sigma_h\|_0 + \|u - P_h u\|_0) \\
&\le Ch(\|u\|_2 + \|\sigma\|_2).
\end{aligned}
$$

That completes the proof of this theorem. ∎

5. The minimal element in any spatial dimension

Assume the domain Ω is a unit hypercube $[0,1]^n$ in the n-dimensional space, which is subdivided by a uniform rectangular grid of N^n cubes:

$$
\begin{aligned}
\mathcal{T}_h := \{K_{i_1,i_2,\ldots,i_n} = [(i_1-1)h, i_1 h] \times \cdots [(i_n-1)h, i_n h],\\
1 \le i_1, \cdots i_n \le N;\ h = 1/N\}.
\end{aligned}
$$

The set of all $(n-1)$-dimensional face hyperplanes of the triangulation $\mathcal{T}_h$ that are perpendicular to the axis x_i is denoted by $\mathcal{E}_{n-1,i}$. That is

$$
\begin{aligned}
\mathcal{E}_{n-1,i} = \{[(i_1-1)h, i_1 h] \times \cdots \times [(i_{i-1}-1)h, i_{i-1}h] \times \{i_i h\}\\
\times \cdots \times [(i_n-1)h, i_n h],\ 1 \le i_1, \cdots i_n \le N,\ 0 \le i_i \le N\}.
\end{aligned}
$$

The internal hyperplanes are denoted by

$$\mathcal{E}_{n-1,i}(\Omega) = \mathcal{E}_{n-1,i} \cap \Omega.$$

The set of all $(n-2)$-dimensional mid-surface hyperplanes (orthogonal to both x_i and x_j axes) are denoted by

$$
\begin{aligned}
\mathcal{E}_{n-2,ij} = \{&[(i_1-1)h, i_1 h] \times \cdots \times \{i_i h\} \times \cdots \times \{(i_j - \tfrac{1}{2})h\} \times \cdots \times \\
&[(i_n-1)h, i_n h],\ 1 \le i_1, \cdots i_n \le N,\ 0 \le i_i \le N\} \\
\cup \{&[(i_1-1)h, i_1 h] \times \cdots \times \{(i_i - \tfrac{1}{2})h\} \times \cdots \times \{i_j h\} \times \cdots \times \\
&[(i_n-1)h, i_n h],\ 1 \le i_1, \cdots i_n \le N,\ 0 \le i_i \le N\}.
\end{aligned}
$$

In addition, define $\mathcal{E}_{n-2,ij}(K) := \mathcal{E}_{n-2,ij} \cap \partial K$ for any $K \in \mathcal{T}_h$. In 2D, these sets are

$$\begin{aligned}\mathcal{E}_{1,1} &= \{\text{all edges in } \mathcal{T}_h \text{ perpendicular to } x_1 \},\\ \mathcal{E}_{1,2} &= \{\text{all edges in } \mathcal{T}_h \text{ perpendicular to } x_2 \},\\ \mathcal{E}_{0,12} &= \{\text{all mid-points of edges in } \mathcal{T}_h \}.\end{aligned}$$

In 3D, they are

$$\begin{aligned}\mathcal{E}_{2,i} &= \{\text{all squares in } \mathcal{T}_h \text{ perpendicular to } x_i \},\ 1 \le i \le 3,\\ \mathcal{E}_{1,ij} &= \{\text{all mid-square edges of squares in } \mathcal{E}_{2,i} \text{ and } \mathcal{E}_{2,j},\\ &\qquad \text{parallel to } x_k \},\ i \neq j \neq k \in \{1,2,3\}.\end{aligned}$$

In n space-dimension, the symmetric tensor space is defined in (1.2). The discrete stress space is defined by

$$\begin{aligned}\Sigma_h := \Big\{ \left(\tau_{ij}\right)_{n\times n} \in L^2(\Omega, \mathbb{R}^{n\times n}) \ \Big| \ &\tau_{ij} = \tau_{ji};\\ &\tau_{ii}|_K \in \operatorname{span}\{1, x_i\}, \tau_{ii} \text{ is continuous on } E_i \in \mathcal{E}_{n-1,i};\\ &\tau_{ij}|_K \in \operatorname{span}\{1, x_i, x_j\},\ \tau_{ij} \text{ is continuous on } E_{ij} \in \mathcal{E}_{n-2,ij}(\Omega)\Big\}.\end{aligned} \tag{5.1}$$

Some comments are in order for this family of minimal finite element spaces.

Remark 5.1. *The normal stress τ_{ii} is a constant on each $(n-1)$-dimensional hyper-plane $E_i \in \mathcal{E}_{n-1,i}$. In addition, for the case $n = 1$, Σ_h is*

$$\{\tau_{11} \in L^2(\Omega, \mathbb{R}) \ \big| \ \tau|_K \in \mathit{span}\{1, x\} \ \textit{is continuous at the nodes} \ \} \subset H^1(\Omega),$$

the 1D Raviart-Thomas space, which is the only conforming space in this family.

Remark 5.2. *The dimension of the space*

$$\begin{aligned}\Sigma_{h,ij} := \{\tau_{ij} \in L^2(\Omega, \mathbb{R}) \ \big| \ &\tau_{ij}|_K \in \operatorname{span}\{1, x_i, x_j\},\\ &\tau_{ij} \ \textit{is continuous on } E_{ij} \in \mathcal{E}_{n-2,ij}(\Omega)\}\end{aligned}$$

is

$$N^{n-2}((n+1)^2 - 1) = N^n + 2N^{n-1}.$$

see [25] *for more details for 2D.*

Let us give the local basis for τ_{ii} and but a local frame (not basis) for τ_{ij} on an element $K := K_{i_1,i_2,\ldots,i_n} \in \mathcal{T}_h$. Define, for $(x_1, \ldots, x_n) \in K$,

$$\psi_{ii,K}^{(k)}(x_1, \ldots, x_n) = \hat{\psi}^{(k)}\left(\frac{x_i - (i_i - 1/2)h}{h/2}\right), \quad k = 0, 1,$$

where

$$\hat{\psi}^{(0)}(\hat{x}) = \frac{1-\hat{x}}{2}, \qquad \hat{\psi}^{(1)}(\hat{x}) = \frac{1+\hat{x}}{2}, \qquad \hat{x} \in [-1, 1].$$

Define, for $k = 0, 1, 2, 3$, for $(x_1, \ldots, x_n) \in K$,

$$\phi_{ij,K}^{(k)}(x_1, \ldots, x_n) = \hat{\phi}^{(k)}\left(\frac{x_i - (i_i - 1/2)h}{h/2}, \frac{x_j - (i_j - 1/2)h}{h/2}\right),$$

where (cf. Figure 3), for $(\hat{x}, \hat{y}) \in [-1, 1]^2$,

$$\begin{aligned}\hat{\phi}^{(0)}(\hat{x}, \hat{y}) &= \frac{1 - \hat{x} - \hat{y}}{4}, & \hat{\phi}^{(1)}(\hat{x}, \hat{y}) &= \frac{1 + \hat{x} - \hat{y}}{4},\\ \hat{\phi}^{(2)}(\hat{x}, \hat{y}) &= \frac{1 + \hat{x} + \hat{y}}{4}, & \hat{\phi}^{(3)}(\hat{x}, \hat{y}) &= \frac{1 - \hat{x} + \hat{y}}{4}.\end{aligned}$$

Note that the above four functions are not linearly independent. In fact,

$$\hat{\phi}^{(0)} - \hat{\phi}^{(1)} + \hat{\phi}^{(2)} - \hat{\phi}^{(3)} \equiv 0.$$

Then the finite element space can be alternatively defined by

$$\begin{aligned}\Sigma_h = \Big\{ \left(\tau_{ij}\right)_{n\times n} \in L^2(\Omega, \mathbb{R}^{n\times n}) \;\Big|\; &\tau_{ij} = \tau_{ji};\\ \tau_{ii}|_K = &\sum_{k=0}^{1} \tau_{ii}(E^{(k)}_{n-1,i}(K))\psi^{(k)}_{ii,K}(x_1,\ldots,x_n);\\ \tau_{ij}|_K = &\sum_{k=0}^{3} p_{ij}(\hat{E}^{(k)}_{n-2}(K))\phi^{(k)}_{ij,K}(x_1,\ldots,x_n)\Big\}.\end{aligned} \tag{5.2}$$

Here $\tau_{ii}(\hat{E}^{(k)}_{n-1,i}(K))$ are the values of τ_{ii} at the centers of the $(n-1)$-dimensional hyperplanes of $K = K_{i_1,\cdots,i_n}$:

$$\hat{E}^{(k)}_{n-1,i}(K) = \begin{pmatrix} (i_1 - \frac{1}{2})h \\ \vdots \\ (i_{i-1} - \frac{1}{2})h \\ (i_i - k)h \\ \vdots \\ (i_n - \frac{1}{2})h \end{pmatrix}, \; k = 0, 1;$$

$p_{ij}(\hat{E}^{(k)}_{n-2}(K)) \in \mathbb{R}$ are some parameters associated to the center-point of four $(n-2)$-dimensional hyperplanes of K which are continuous on the four (two on the boundary) n-cubes sharing the point:

$$\hat{E}^{(k)}_{n-2}(K) = \begin{pmatrix} (i_1 - \frac{1}{2})h \\ \vdots \\ (i_i - 0)h \\ \vdots \\ (i_j - 0)h \\ \vdots \\ (i_n - \frac{1}{2})h \end{pmatrix}, \begin{pmatrix} (i_1 - \frac{1}{2})h \\ \vdots \\ (i_i - 1)h \\ \vdots \\ (i_j - 0)h \\ \vdots \\ (i_n - \frac{1}{2})h \end{pmatrix}, \begin{pmatrix} (i_1 - \frac{1}{2})h \\ \vdots \\ (i_i - 1)h \\ \vdots \\ (i_j - 1)h \\ \vdots \\ (i_n - \frac{1}{2})h \end{pmatrix}, \begin{pmatrix} (i_1 - \frac{1}{2})h \\ \vdots \\ (i_i - 0)h \\ \vdots \\ (i_j - 1)h \\ \vdots \\ (i_n - \frac{1}{2})h \end{pmatrix}.$$

As in 2D, the discrete displacement space is

$$V_h = \{v \in L^2(\Omega, \mathbb{R}^n) \mid v|_K \text{ is a constant vector }\}. \tag{5.3}$$

In particular, the dof of the 3D mixed element is plotted in Figure 2.

In the n-dimension, since $\operatorname{div}_h \Sigma_h \subset V_h$, the K-ellipticity (3.1) is proved exactly the same way as in 2D. The explicit construction proof of the discrete B-B condition (3.2) can be divided into n essentially 1-dimensional construction proofs similar to that for the 1D Raviart-Thomas element of the 1D Poisson equation, see Section 3 for more details for 2D. For the consistency error in (4.15), the proof remains the same except there is a multiple summation instead of 2-index summation. All the analysis in 2D remains the same for n-D.

6. The pure traction problem

This section considers the pure traction problem, i.e., the stress space is subject to zero Neumann boundary condition while no boundary condition on the displacement. In practice, part of elasticity body should be located, i.e, the displacement has a Dirichlet boundary condition on some non-zero measure boundary. But the pure traction problem is the most difficult one in mathematical analysis. A similar proof for Theorem 6.1 can prove it for partial displacement problems. For ease of presentation, details are

presented only for two dimensions. Note that the argument in any dimension is similar. The main idea is to use the macro-element technique where we construct a mass-preserving quasi-interpolation operator.

Let RM be the rigid motion space in two dimensions, which reads

$$\mathrm{RM} := \mathrm{span}\left\{ \begin{pmatrix}1\\0\end{pmatrix}, \begin{pmatrix}0\\1\end{pmatrix}, \begin{pmatrix}y\\-x\end{pmatrix} \right\}.$$

Consider a pure traction problem:

$$\operatorname{div}(A^{-1}\epsilon(u)) = f \quad \text{in } \Omega = (0,1)^2, \tag{6.1a}$$

$$\epsilon(u)\cdot n = 0 \quad \text{on } \Gamma = \partial\Omega, \tag{6.1b}$$

$$(u, v) = 0 \quad \forall v \in \mathrm{RM}. \tag{6.1c}$$

By the same discretization of uniform square grid $\mathcal{T}_h$ with $h = 1/N$ as in §2, the finite element equations (2.6) remain the same except the spaces are changed with boundary and rigid-motion free conditions:

$$\begin{aligned} (A\sigma_h, \tau) + (\operatorname{div}_h \tau, u_h) &= 0 \qquad \forall \tau \in \Sigma_{h,0}, \\ (\operatorname{div}_h \sigma_h, v) &= (f, v) \quad \forall v \in V_{h,0}, \end{aligned}$$

where

$$\Sigma_{h,0} = \{\sigma = \begin{pmatrix}\sigma_{11} & \sigma_{12}\\ \sigma_{12} & \sigma_{22}\end{pmatrix} \in \Sigma_h \mid \sigma(m_e)\cdot n = 0 \quad \forall e \in (\mathcal{E}_h \cap \Gamma)\}, \tag{6.2}$$

$$V_{h,0} = \{v = \begin{pmatrix}v_1\\ v_2\end{pmatrix} \in V_h \mid \ (v, w) = 0 \quad \forall w \in \mathrm{RM}\}. \tag{6.3}$$

Here m_e is the mid-point of an edge e, and Σ_h and V_h are defined in (2.4) and (2.5), respectively. The earlier analysis remains the same except the discrete B-B condition (3.2) as the stress space $\Sigma_{h,0}$ is much smaller than before.

Theorem 6.1. *The following discrete B-B condition holds uniformly,*

$$\inf_{v_h \in V_{h,0}} \sup_{\sigma_h \in \Sigma_{h,0}} \frac{(\operatorname{div}_h \sigma_h, v_h)}{\|\sigma_h\|_{H(\operatorname{div}_h)} \|v_h\|_0} \ge C.$$

Proof. Let $v_h = ((v_h)_1, (v_h)_2) = \sum (v_h)_{ij}\varphi_{ij}$ as in (3.3), where $(v_h)_{ij} = ((v_h)_{1,ij}, (v_h)_{2,ij})$ is the constant value of v_h on square K_{ij}. With the boundary condition on the stress, it is impossible to match $(v_h)_1$ by $\partial_x \tau_{11}$ alone as in (3.4). That is, because the dof of $(v_h)_1$ is $n^2 - 1.5$ (due to a mixed constraint with the second component $(v_h)_2$), but the dof of $\{\tau_{11}\}$ is only $n(n-1)$. This indicates that the help from $\partial_y \tau_{12}$ is indispensable. But the traditional trick of interpolating smooth B-B stress function does not work here as (τ_{12}) does not have enough dof. In other words, the support of τ_{21} is non-local, at least on four neighboring squares. Given v_h, a discrete B-B stress function will be constructed in two steps. First, a macro-element technique will produce a $\tilde{\sigma}_h$ globally so that $v_h - \operatorname{div}_h \tilde{\sigma}_h$ is rigid-motion free on each (2×2) macro-element $K_{2i,2j,2h} := [x_{2i}, x_{2i+2}] \times [y_{2j}, y_{2j+2}]$. In a second step, construct, macro-element by macro-element, a $\bar{\sigma}_h$ locally by internal dof only, so that $\operatorname{div}_h \bar{\sigma}_h = v_h - \operatorname{div}_h \tilde{\sigma}_h$.

To this end, define a local rigid-motion space on each macro-element $K_{2i,2j,2h}$

$$R_{ij} = \mathrm{span}\{\phi^r_{1,ij}, \phi^r_{2,ij}, \phi^r_{3,ij}\}, \tag{6.4}$$

where $\phi^r_{1,ij}$ are defined in Figure 5, piecewise constant functions. Assume N is an even integer and decompose v_h into two parts, a local rigid-motion and a global rigid-motion-free part,

$$v_h = \tilde{v}_h + \bar{v}_h, \quad \tilde{v}_h = P_{L^2(R_{ij})} v_h \ \text{ for } 0 \le i, j \le N/2 - 1. \tag{6.5}$$

Here the projection $P_{L^2(R_{ij})} v_h$ is defined as

$$\int_{K_{2i,2j,2h}} P_{L^2(R_{ij})} v_h \cdot \phi^r_{m,ij}\, dx\, dy = \int_{K_{2i,2j,2h}} v_h \cdot \phi^r_{m,ij}\, dx\, dy, \quad m = 1, 2, 3.$$

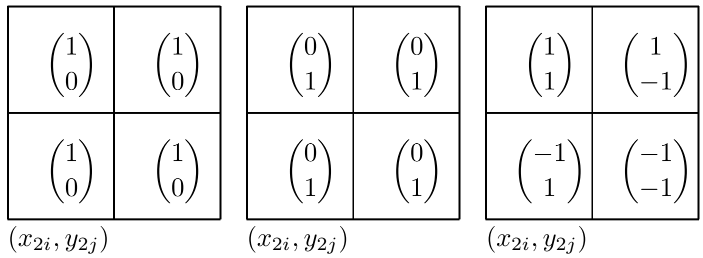

FIGURE 5. Nodal values of three orthogonal basis functions, $\{\phi^r_{m,ij}, m = 1, 2, 3\}$, of the rigid-motion space on macro-element $K_{2i,2j,2h} := [x_{2i}, x_{2i+2}] \times [y_{2j}, y_{2j+2}]$, cf. (6.4).

To construct $\tilde{\sigma}_h$, consider the pure traction PDE (6.1a) with $f = \tilde{v}_h$ with the solution $u \in H^2(\Omega)$. Let

$$\sigma = A^{-1}\epsilon(u) \in H^1(\Omega).$$

Then

$$\operatorname{div} \sigma = \tilde{v}_h, \quad \|\sigma\|_{H(\mathrm{div})} \le C\|\tilde{v}_h\|_0. \tag{6.6}$$

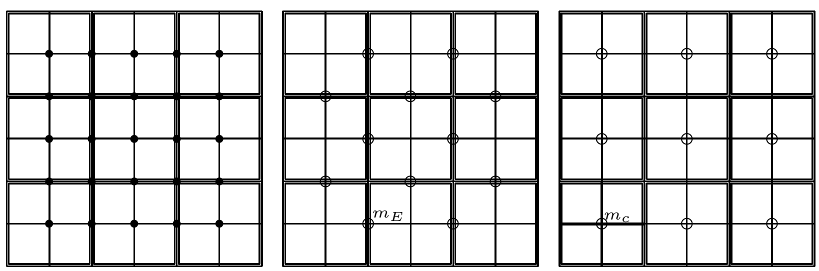

FIGURE 6. Interpolation nodes for the Scott-Zhang C^0-Q_1 I_h, I_h^E, cf. (6.7) and I_h^c, cf. (6.8).

For the analysis, we need a mass-preserving quasi-interpolation operator. This will be achieved in four steps. First, let I_h be the boundary-condition preserving Scott-Zhang operator from [26], which interpolates H_0^1 functions to $C_0^0(\Omega)$-$Q_1(\mathcal{T}_h)$ functions, shown in Figure 6. Then, we correct the mid-point values of edges of macro-elements to get a mass-preserving on each edge of each macro-element $K_{2i,2j,2h}$. Let m_E be the mid-point of edge E of $K_{2i,2j,2h}$, which is also a vertex of $\mathcal{T}_h$, define the associated nodal basis function of the conforming bilinear element by

$$\theta_E(m_E) = 1, \quad \theta_E(q) = 0 \text{ for other vertexes } q \text{ of } \mathcal{T}_h.$$

Let

$$c_E = \int_E (v - I_h v)ds \Big/ \int_E \theta_E ds.$$

Define $I_h^E : H_0^1(\Omega) \to C_0^0(\Omega)$-$Q_1(\mathcal{T}_h)$ by

$$I_h^E v = I_h v + \sum_E c_E \theta_E. \tag{6.7}$$

Third, we correct the center value of $I_h^E v$ on each macro-element. Let m_c be the center of macro-element $K_{2i,2j,2h}$, which is also a vertex of $\mathcal{T}_h$. Let the Q_1 nodal basis function θ_{ij} for vertex m_c be similarly defined as θ_E. Define

$$c_{ij} = \Big(\int_{E_{1,ij}} (v - I_{2,h}v)ds + \int_{E_{2,ij}} (v - I_{2,h}v)ds\Big) \Big/ \Big(\int_{E_{1,ij}} \theta_{ij} ds + \int_{E_{2,ij}} \theta_{ij} ds\Big),$$

where $E_{1,ij} = [x_{2i}, x_{2i+2}] \times \{y_{2j+1}\}$ and $E_{2,ij} = \{x_{2i+1}\} \times [y_{2j}, y_{2j+2}]$ are two intervals in the interior of $K_{2i,2j,2h}$ that take m_c as their mid-points, cf. Figure 6. Define $I_h^c : H_0^1(\Omega) \to C_0^0(\Omega)\text{-}Q_1(\mathcal{T}_h)$ by

$$I_h^c v = I_h^E v + \sum_{ij} c_{ij}\theta_{ij}. \tag{6.8}$$

Finally, define $\tilde{\Pi}_{12} : H_0^1(\Omega) \to W_{h,0} := \{w \in W_h | \quad w(m_e) = 0 \ \forall e \in \mathcal{E}_h \cap \Gamma\}$ by

$$\tilde{\Pi}_{12} v := \Pi_{12} I_h^c v \text{ for any } v \in H_0^1(\Omega). \tag{6.9}$$

Since $\int_e \Pi_{12} I_h^c v ds = \int_e I_h^c v ds$ for any $e \in \mathcal{E}_h$, the definition of the interpolation operator $\tilde{\Pi}_{12}$ leads to

$$\int_E \tilde{\Pi}_{12} v ds = \int_E v ds \text{ and } \int_{E_{1,ij}} (v - \tilde{\Pi}_{12} v) ds + \int_{E_{2,ij}} (v - \tilde{\Pi}_{12} v) ds = 0, \tag{6.10}$$

for any $E \subset \partial K_{2i,2j,2h}$ and any macro-element $K_{2i,2j,2h}$. In addition,

$$\|\nabla_h \tilde{\Pi}_{12} v\|_0 \le C \|\nabla v\|_0. \tag{6.11}$$

Then $\tilde{\sigma}_h$ is defined as

$$\tilde{\sigma}_{11} = \Pi_{11}\sigma_{11}, \tag{6.12}$$
$$\tilde{\sigma}_{22} = \Pi_{22}\sigma_{22}, \tag{6.13}$$
$$\tilde{\sigma}_{12} = \tilde{\Pi}_{12}\sigma_{12}, \tag{6.14}$$

where Π_{11}, Π_{22} and $\tilde{\Pi}_{12}$ are defined in (4.2), (4.3) and (6.9), respectively.

We verify next, for $\tilde{\sigma}_h$ defined in (6.12)–(6.14),

$$\int_{K_{2i,2j,2h}} (\operatorname{div}_h \tilde{\sigma}_h - v_h) \cdot \phi_{m,ij}^r dx\, dy = 0, \quad m = 1, 2, 3,$$

for $0 \le i, j < N/2$. Note that $\operatorname{div}_h \tilde{\sigma}_h \ne \tilde{v}_h$ in general, though $\operatorname{div} \sigma = \tilde{v}_h$. From (4.2), (4.3), (6.9) and (6.10), and integrations by parts it follows

$$\begin{aligned} &\int_{x_{2i}}^{x_{2i+2}} \int_{y_{2j}}^{y_{2j+2}} \operatorname{div}_h(\sigma - \tilde{\sigma}_h) \cdot \phi_{1,ij}^r dy\, dx \\ &= \int_{y_{2j}}^{y_{2j+2}} (I - \Pi_{11})[\sigma_{11}(x_{2i+2}, y) - \sigma_{11}(x_{2i}, y)]\, dy \\ &\quad + \int_{x_{2i}}^{x_{2i+2}} (I - \tilde{\Pi}_{12})[\sigma_{12}(x, y_{2j+2}) - \sigma_{12}(x, y_{2j})]\, dx = 0. \end{aligned}$$

Symmetrically,

$$\int_{x_{2i}}^{x_{2i+2}} \int_{y_{2j}}^{y_{2j+2}} \operatorname{div}_h(\sigma - \sigma_h) \cdot \phi_{2,ij}^r dy\, dx = 0.$$

For the last preserved value, as $\operatorname{div}\sigma = \tilde{v}_h$ pointwise, from (4.2), (4.3), (6.9) and (6.10), and integrations by parts it follows

$$
\begin{aligned}
&\int_{x_{2i}}^{x_{2i+2}}\int_{y_{2j}}^{y_{2j+2}} \operatorname{div}_h(\sigma-\tilde{\sigma}_h)\cdot\phi^r_{3,ij}\,dy\,dx\\
=&\int_{y_{2j+1}}^{y_{2j+2}}(I-\Pi_{11})[\sigma_{11}(x_{2i+2},y)-\sigma_{11}(x_{2i},y)]\,dy\\
&\quad-\int_{y_{2j}}^{y_{2j+1}}(I-\Pi_{11})[\sigma_{11}(x_{2i+2},y)-\sigma_{11}(x_{2i},y)]\,dy\\
&\quad+\int_{x_{2i}}^{x_{2i+1}}(I-\Pi_{22})[\sigma_{22}(x,y_{2j+2})-\sigma_{22}(x,y_{2j})]\,dx\\
&\quad-\int_{x_{2i+1}}^{x_{2i+2}}(I-\Pi_{22})[\sigma_{22}(x,y_{2j+2})-\sigma_{22}(x,y_{2j})]\,dx\\
&\quad+\int_{x_{2i}}^{x_{2i+2}}(I-\tilde{\Pi}_{12})[\sigma_{12}(x,y_{2j+2})+\sigma_{12}(x,y_{2j})-2\sigma_{12}(x,y_{2j+1})]\,dx\\
&\quad+\int_{y_{2j}}^{y_{2j+2}}(I-\tilde{\Pi}_{12})[2\sigma_{12}(x_{2i+1},y)-\sigma_{12}(x_{2i+2},y)-\sigma_{12}(x_{2i},y)]\,dy=0\,.
\end{aligned}
$$

Thus

$$
\Big[v_h-\operatorname{div}_h\tilde{\sigma}_h\Big]_{K_{2i,2j,2h}}\perp R_{ij}\quad 0\le i,j<N/2.
$$

We match next $[v_h-\operatorname{div}_h\tilde{\sigma}_h]$ on each macro-element $K_{2i,2j,2h}$ by the divergence of internal 5 dof of discrete stress:

$$
\bar{\sigma}_{11,2i+1,2j+\frac12},\ \bar{\sigma}_{11,2i+1,2j+\frac32},\ \bar{\sigma}_{12,2i+1,2j+\frac12},\ \bar{\sigma}_{22,2i+\frac12,2j+1}\ \text{ and }\bar{\sigma}_{22,2i+\frac32,2j+1},
$$

where $\bar{\sigma}_{11,2i+1,2j+\frac12}$ denotes the value of $\bar{\sigma}_{11}$ at $((2i+1)h,(2j+\frac12)h)$ and other notations are defined similarly. Note that the four mid-edge values of $\bar{\sigma}_{12}$ are the same. Here on each macro-element, $[v_h-\operatorname{div}_h\tilde{\sigma}_h]$ is in the following space

$$
M_{ij}=\operatorname{span}\{\phi^c_{m,ij},\ m=1,2,3,4,5\} \tag{6.15}
$$

where $\phi^c_{m,ij}$ are defined in Figure 7.

$$
\begin{array}{|c|c|}\hline \begin{pmatrix}0\\0\end{pmatrix} & \begin{pmatrix}0\\0\end{pmatrix}\\\hline \begin{pmatrix}-1\\0\end{pmatrix} & \begin{pmatrix}1\\0\end{pmatrix}\\\hline\end{array}\quad
\begin{array}{|c|c|}\hline \begin{pmatrix}1\\0\end{pmatrix} & \begin{pmatrix}-1\\0\end{pmatrix}\\\hline \begin{pmatrix}0\\0\end{pmatrix} & \begin{pmatrix}0\\0\end{pmatrix}\\\hline\end{array}\quad
\begin{array}{|c|c|}\hline \begin{pmatrix}0\\0\end{pmatrix} & \begin{pmatrix}1\\0\end{pmatrix}\\\hline \begin{pmatrix}-1\\-1\end{pmatrix} & \begin{pmatrix}0\\1\end{pmatrix}\\\hline\end{array}\quad
\begin{array}{|c|c|}\hline \begin{pmatrix}0\\0\end{pmatrix} & \begin{pmatrix}1\\1\end{pmatrix}\\\hline \begin{pmatrix}-1\\-1\end{pmatrix} & \begin{pmatrix}0\\0\end{pmatrix}\\\hline\end{array}\quad
\begin{array}{|c|c|}\hline \begin{pmatrix}0\\1\end{pmatrix} & \begin{pmatrix}0\\0\end{pmatrix}\\\hline \begin{pmatrix}0\\-1\end{pmatrix} & \begin{pmatrix}0\\0\end{pmatrix}\\\hline\end{array}
$$

FIGURE 7. Nodal values of basis functions $\{\phi^c_{m,ij},\ 1\le m\le 5\}$ in M_{ij} on macro-element $x_{2i}\le x\le x_{2i+2}$, $y_{2j}\le y\le y_{2j+2}$, cf. (6.15).

On each macro-element, define 5 stress functions to match the 5 basis functions of M_{ij} such that

$$
\operatorname{div}_h\sigma_{m,ij}=\phi^c_{m,ij}.
$$

Each such a function is denoted by a vector of its nodal values:

$$\frac{1}{h}\sigma_{m,ij} = \begin{pmatrix} \bar\sigma_{11,2i+1,2j+1/2} \\ \bar\sigma_{11,2i+1,2j+3/2} \\ \bar\sigma_{12,2i+1/2,2j+1/2} \\ \bar\sigma_{22,2i+1/2,2j+1} \\ \bar\sigma_{22,2i+3/2,2j+1} \end{pmatrix} = \begin{pmatrix} -1 \\ 0 \\ 0 \\ 0 \\ 0 \end{pmatrix}, \begin{pmatrix} 0 \\ 1 \\ 0 \\ 0 \\ 0 \end{pmatrix}, \frac{1}{2}\begin{pmatrix} -1 \\ -1 \\ -1 \\ -1 \\ 1 \end{pmatrix}, \frac{1}{2}\begin{pmatrix} -1 \\ -1 \\ -1 \\ -1 \\ -1 \end{pmatrix}, \frac{1}{2}\begin{pmatrix} 0 \\ 0 \\ 0 \\ -1 \\ 0 \end{pmatrix},$$

for $1 \le m \le 5$. A linear expansion $\left[v_h - \operatorname{div}_h \tilde\sigma_h\right]_{K_{2i,2j,2h}} = \sum_{m=1}^{5} c_{m,ij}\phi^c_{m,ij}$ defines $\bar\sigma_h(x,y)$ by

$$\bar\sigma_h(x,y) = \sum_{m=1}^{5} c_{m,ij}\sigma_{m,ij}, \quad (x,y) \in K_{2i,2j,2h}.$$

Thus

$$\operatorname{div}_h \bar\sigma_h = v_h - \operatorname{div}_h \tilde\sigma_h \text{ and } \|\bar\sigma_h\|_0 \le C\|v_h\|_0. \tag{6.16}$$

This stability is obtained by the standard scaling argument as all norms on 5-dimensional space M_{ij} are equivalent.

The final σ_h for v_h is defined as

$$\sigma_h = \bar\sigma_h + \tilde\sigma_h.$$

As $\operatorname{div}_h \sigma_h = v_h$, by (6.11) and (6.16), the discrete B-B condition holds uniformly. ∎

7. Numerical tests

Two examples in 2D and one in 3D are presented to demonstrate the methods. These are pure displacement problem with a homogeneous boundary condition that $u \equiv 0$ on $\partial\Omega$. Assume the material is isotropic in the sense that

$$A\sigma = \frac{1}{2\mu}\left(\sigma - \frac{\lambda}{2\mu + n\lambda}\operatorname{tr}(\sigma)\delta\right), \quad n = 2, 3, \tag{7.1}$$

where $\delta = \begin{pmatrix} 1 & 0 \\ 0 & 1 \end{pmatrix}$, and μ and λ are the Lamé constants such that $0 < \mu_1 \le \mu \le \mu_2$ and $0 < \lambda < \infty$.

In 2D, let the exact solution on the unit square $[0,1]^2$ be

$$u = \begin{pmatrix} 4x(1-x)y(1-y) \\ -4x(1-x)y(1-y) \end{pmatrix}, \tag{7.2}$$

and

$$u = \begin{pmatrix} e^{x-y}x(1-x)y(1-y) \\ \sin(\pi x)\sin(\pi y) \end{pmatrix}. \tag{7.3}$$

Notice that the second example is from [31].

In 2D, the parameters in (7.1) are chosen as

$$\lambda = 1 \quad \text{and} \quad \mu = \frac{1}{2}.$$

Then, the true stress function σ and the load function f are defined by the equations in (1.1), for the given solution u.

In the computation, the level one grid is the given domain, a unit square or a unit cube. Each grid is refined into a half-size grid uniformly, to get a higher level grid, see the first column in Table 1. In Table 1, the errors and the convergence order in various norms are listed for the true solution (7.2). Here and in rest tables in the section, I_h is the usual nodal interpolation operator. For example, $I_h u_1(x_i + h/2, y_j + h/2) = u_1(x_i + h/2, y_j + h/2)$, $I_h\sigma_{11}(x_i, y_j + h/2) = \sigma_{11}(x_i, y_j + h/2)$, and $I_h\sigma_{12} = \Pi_{12}\sigma_{12}$, defined in (2.9). An

TABLE 1. The error and the order of convergence, for (7.2).

	$\Vert I_h u - u_h\Vert_0$	h^n	$\Vert I_h\sigma - \sigma_h\Vert_0$	h^n	$\Vert \operatorname{div}(I_h\sigma - \sigma_h)\Vert_0$	h^n
1	0.05893	0.0	0.72887	0.0	1.41421356	0.0
2	0.02447	1.3	0.24585	1.6	0.35355339	2.0
3	0.00714	1.8	0.06587	1.9	0.08838835	2.0
4	0.00190	1.9	0.01708	1.9	0.02209709	2.0
5	0.00048	2.0	0.00440	2.0	0.00552427	2.0
6	0.00012	2.0	0.00113	2.0	0.00138106	2.0
7	0.00003	2.0	0.00029	2.0	0.00034526	2.0

order 2 convergence is observed for both displacement and stress, see Table 1. However, Theorem 4.3 only shows the first order convergence. Further studies on this superconvergence should be performed.

The next example, (7.3), of Yi [31] is implemented for a comparison. The finite element errors and the order of convergence are listed in Table 2. An order 2 convergence is again observed. Notice that, see Figure 1, the minimal element of this paper has a much less dof than that of Yi, but has one order higher of convergence.

TABLE 2. The error and the order of convergence, for (7.3).

	$\Vert I_h u - u_h\Vert_0$	h^n	$\Vert I_h\sigma - \sigma_h\Vert_0$	h^n	$\Vert \operatorname{div}(I_h\sigma - \sigma_h)\Vert_0$	h^n
1	0.03619	0.0	3.08021	0.0	12.20143741	0.0
2	0.09843	0.0	0.54275	2.5	2.36338456	2.4
3	0.02594	1.9	0.15169	1.8	0.63139891	1.9
4	0.00664	2.0	0.03964	1.9	0.16050210	2.0
5	0.00167	2.0	0.01014	2.0	0.04029305	2.0
6	0.00042	2.0	0.00258	2.0	0.01008376	2.0

As a third example, we compute a 3D solution for the following exact solution:

$$u = \begin{pmatrix} 16x(1-x)y(1-y)z(1-z) \\ 32x(1-x)y(1-y)z(1-z) \\ 64x(1-x)y(1-y)z(1-z) \end{pmatrix}, \tag{7.4}$$

on the unit cube $[0,1]^3$. This time, the parameters in (7.1) are taken as

$$\lambda = 1, \quad \mu = \frac{1}{2} \text{ and } n = 3.$$

Again the order of convergence is still one higher than what is proved in this paper, see Table 3.

TABLE 3. The error and convergence in 3D, for (7.4).

	$\Vert I_h u - u_h\Vert_0$	h^n	$\Vert I_h\sigma - \sigma_h\Vert_0$	h^n	$\Vert \operatorname{div}(I_h\sigma - \sigma_h)\Vert_0$	h^n
1	0.16366	0.0	3.64496	0.0	8.94883415	0.0
2	0.07716	1.1	0.89446	2.0	1.73418255	2.4
3	0.02332	1.7	0.23153	1.9	0.42577123	2.0
4	0.00628	1.9	0.05946	2.0	0.10668050	2.0
5	0.00161	2.0	0.01518	2.0	0.02628774	2.0

As the last example, we compute the pure traction problem (6.1a) with the exact solution

$$u = \left[100x^2(1-x)^2y^2(1-y)^2 - \frac{1}{9}\right]\begin{pmatrix}1\\-1\end{pmatrix}. \tag{7.5}$$

The matrix A is same as that in the first two examples. Our new finite element has no problem in solving the pure traction problems. The convergence results are listed in Table 4.

TABLE 4. The errors and the order of convergence for the pure traction problem (7.5).

	$\|I_h u - u_h\|_0$	h^n	$\|I_h\sigma - \sigma_h\|_0$	h^n	$\|\operatorname{div}(I_h\sigma - \sigma_h)\|_0$	h^n
2	0.41470	0.0	1.19604	0.0	4.14320380	0.0
3	0.12546	1.7	0.26426	2.2	1.10584856	1.9
4	0.03273	1.9	0.06572	2.0	0.28799493	1.9
5	0.00827	2.0	0.01648	2.0	0.07297595	2.0
6	0.00207	2.0	0.00412	2.0	0.01830958	2.0
7	0.00052	2.0	0.00103	2.0	0.00458156	2.0

REFERENCES

[1] S. Adams and B. Cockburn, A mixed finite element method for elasticity in three dimensions, J. Sci. Comput. 25 (2005), no. 3, 515–521.

[2] M. Amara and J. M. Thomas, Equilibrium finite elements for the linear elastic problem, Numer. Math. 33 (1979), 367–383.

[3] D. N. Arnold and G. Awanou, Rectangular mixed finite elements for elasticity, Math. Models Methods Appl. Sci. 15 (2005), 1417–1429.

[4] D. Arnold, G. Awanou and R. Winther, Finite elements for symmetric tensors in three dimensions, Math. Comp. 77 (2008), no. 263, 1229–1251.

[5] D. N. Arnold, F. Brezzi and J. Douglas, Jr., PEERS: A new mixed finite element for plane elasticity, Jpn. J. Appl. Math. 1 (1984), 347–367.

[6] D. N. Arnold, J. Douglas Jr., and C. P. Gupta, A family of higher order mixed finite element methods for plane elasticity, Numer. Math. 45 (1984), 1–22.

[7] D.N. Arnold, R. Falk and R. Winther, Mixed finite element methods for linear elasticity with weakly imposed symmetry, Math. Comp. 76 (2007), no. 260, 1699?1723.

[8] D. N. Arnold and R.Winther, Mixed finite element for elasticity, Numer. Math. 92 (2002), 401–419.

[9] D. N. Arnold and R. Winther, Nonconforming mixed elements for elasticity, Math. Models. Methods Appl. Sci. 13 (2003), 295–307.

[10] G. Awanou, Two remarks on rectangular mixed finite elements for elasticity, J. Sci. Comput. 50 (2012), 91–102.

[11] D. Boffi, F. Brezzi and M. Fortin, Reduced symmetry elements in linear elasticity, Commun. Pure Appl. Anal. 8 (2009), no. 1, 95-?21.

[12] F. Brezzi and M. Fortin, Mixed and hybrid finite element methods, Springer, 1991.

[13] C. Carstensen, M. Eigel and J. Gedicke, Computational competition of symmetric mixed FEM in linear elasticity, Comput. Methods Appl. Mech. Engrg. 200 (2011), no. 41-44, 2903–2915.

[14] C. Carstensen, D. Günther, J. Reininghaus, J. Thiele, The Arnold–Winther mixed FEM in linear elasticity. Part I: Implementation and numerical verification, Comput. Methods Appl. Mech. Engrg. 197 (2008) 3014–3023.

[15] S.-C. Chen and Y.-N. Wang, Conforming rectangular mixed finite elements for elasticity, J. Sci. Comput. 47 (2011), no. 1, 93-108.

[16] B. Cockburn, J. Gopalakrishnan and J. Guzmán, A new elasticity element made for enforcing weak stress symmetry, Math. Comp. 79 (2010), no. 271, 1331–1349.

[17] J. Gopalakrishnan and J. Guzmán, Symmetric nonconforming mixed finite elements for linear elasticity, SIAM J. Numer. Anal. 49 (2011), no. 4, 1504–1520.

[18] J. Gopalakrishnan and J. Guzmán, A second elasticity element using the matrix bubble, IMA J. Numer. Anal. 32 (2012), no. 1, 352–372.

[19] J. Guzmán, A unified analysis of several mixed methods for elasticity with weak stress symmetry, J. Sci. Comput. 44 (2010), no. 2, 156–169.

[20] J.Hu and Z.C. Shi, Constrained quadrilateral nonconforming rotated Q_1-element, J. Comp. Math. 23 (2005), 561–586.

[21] J. Hu and Z. C. Shi, Lower order rectangular nonconforming mixed elements for plane elasticity, SIAM J. Numer. Anal. 46 (2007), 88–102.
[22] C. Johnson and B. Mercier, Some equilibrium finite element methods for two-dimensional elasticity problems, Numer.Math. 30 (1978), 103–116.
[23] H.-Y. Man, J. Hu and Z.-C. Shi, Lower order rectangular nonconforming mixed finite element for the three-dimensional elasticity problem, Math. Models Methods Appl. Sci. 19 (2009), no. 1, 51–65.
[24] M. Morley, A family of mixed finite elements for linear elasticity Numer. Math. 55 (1989), no. 6, 633?666.
[25] C. Park and D. Sheen, P1-nonconforming quadrilateral finite element methods for second-order elliptic problems, SIAM J. Numer. Anal. 41 (2003), no. 2, 624–640.
[26] L. R. Scott and S. Zhang, Finite element interpolation of nonsmooth functions satisfying boundary conditions, Math. Comp. 54 (1990), 483–493.
[27] R. Stenberg, On the construction of optimal mixed finite element methods for the linear elasticity problem, Numer. Math. 48 (1986), 447–462.
[28] R. Stenberg, Two low-order mixed methods for the elasticity problem, In: J. R. Whiteman (ed.): The Mathematics of Finite Elements and Applications, VI. London: Academic Press, 1988, 271–280.
[29] R. Stenberg, A family of mixed finite elements for the elasticity problem, Numer. Math. 53 (1988), no. 5, 513–538.
[30] S. Y. Yi, Nonconforming mixed finite element methods for linear elasticity using rectangular elements in two and three dimensions, CALCOLO 42 (2005), 115-133.
[31] S. Y. Yi, A New nonconforming mixed finite element method for linear elasticity, Math. Models Methods Appl. Sci. 16 (2006), 979–999.

LMAM and School of Mathematical Sciences, Peking University, Beijing 100871, P. R. China. hujun@math.pku.edu.cn

Department of Mathematics, Beijing Institute of Technology, Beijing 100081, P. R. China. manhy@bit.edu.cn

Department of Mathematical Sciences, University of Delaware, Newark, DE 19716, USA. szhang@udel.edu